Numerical Analysis of Flow and Pollutant Dispersion over 2-D Bell Shaped Hills

Young-Rae Jung, Keun Park, Warn-Gyu Park*
School of Mechanical Engineering, Pusan National University, Jangjeon-Dong, Kumjeong-Gu, Pusan 609-735, Korea
Ok-Hyun Park
Department of Environmental Engineering, Pusan National University, Pusan 609-735, Korea

The numerical simulations of flow and pollutant particle dispersion are described for two-dimensional bell shaped hills with various aspect ratios. The Reynolds-averaged incompressible Navier-Stokes equations with low Reynolds number k-ε turbulent model are used to simulate the flowfield. The gradient diffusion equation is used to solve the pollutant dispersion field. The code was validated by comparison of velocity, turbulent kinetic energy, Reynolds shear stress, speed-up ratio, and ground level concentration with experimental and numerical data. Good agreement has been achieved and it has been found that the pollutant dispersion pattern and ground level concentration have been strongly influenced by the hill shape and aspect ratio, as well as the location and height of the source.

Key Words: Pollutant Dispersion, Navier-Stokes Equation, Gradient Diffusion Equation, Low-Reynolds Number k-ε Model, Bell Shaped Hill, Ground Level Concentration

1. Introduction

The analysis of pollutant dispersion over the hill has been a matter of practical importance for environmental concerns of wastes incinerating facilities, power plants, industrial complex, etc. A lot of investigations have been performed by experiments using the meteorological wind tunnels. Arya et al. (1987) described the experimental results on the flow and particle dispersion over two-dimensional low height and gentle slope hills of different shapes and aspect ratios. Gong et al. (1989, 1991) experimented the particle dispersion in neutrally stratified flows. In the analysis, most of dispersion models which were widely used for environmental pollution regulation were based on the Gaussian plume model(Robert, 1994). This model is valid only to dispersion over the level ground whose roughness height is less than 0.5 m and restricted to use in the mountainous region because the Gaussian model does not account for the effects of turbulence, recirculating separation flow, and non-uniform shear flow due to terrain topography. Recently, the numerical analysis based on the Navier-Stokes equations has been tried by virtue of computer power and high accurate algorithms. Castro et al. (1997) computed the flow and dispersion over Russian hill using the modified k-ε turbulent model. Kim et al. (1997a, 1997b) presented numerical prediction of pollution dispersion over a hilly terrain using the finite-volume method with standard k-ε turbulent model, especially low Reynolds number k-ε turbulent model for the separated flow. It has been known that the main effects on the dispersion of pollution result from changes in mean flow, turbulence, and the possibility of advection

* Corresponding Author,
E-mail : wgpark@hyowon.cc.pusan.ac.kr
TEL : +82-51-510-2457; **FAX** : +82-51-512-5236
School of Mechanical Engineering, Pusan National University, Jangjeon-Dong, Kumjeong-Gu, Pusan 609-735, Korea. (Manuscript **Received** November 14, 2001; **Revised** February 25, 2003)

into recirculating regions. Because of these effects, choosing a suitable turbulent model and discretizing of convection term are very important for dispersion calculation. As the standard k-ε turbulent model generally uses the wall funtion, the turbulence structure responds to mean flow curvature and longitudinal strains cannot be captured near wall. In this study, a low Reynolds number k-ε turbulent model was used to get over deficiency of the wall funtion and more accurate upwind scheme(SMART) to reduce unphysical oscillations for convective term.

The objective of present work is to modify a computer code of Park et al. (1991, 1993) for predicting atmospheric wind flow field and pollutant particle dispersion over a hilly terrain using the Reynolds averaged Navier-Stokes equation with low Reynolds number k-ε turbulent model and the gradient diffusion theory (K-theory).

2. Mathematical and Numerical Formulation

2.1 Atmospheric flowfield analysis

The unsteady incompressible Navier-Stokes equations in a generalized curvilinear two-dimensional coordinate system may be written as follows;

$$\frac{\partial \hat{q}}{\partial \tau}+\frac{\partial}{\partial \xi}(\hat{E}-\hat{E}_v)+\frac{\partial}{\partial \eta}(\hat{F}-\hat{F}_v)=0 \tag{1}$$

where the flow property vector, $\hat{q}$ and convective flux vectors, $\hat{E}$ are $\hat{F}$ are given as

$$\hat{q}=\frac{1}{J}\begin{bmatrix}0\\ u\\ v\end{bmatrix};\ \hat{E}=\frac{1}{J}\begin{bmatrix}U-\xi_t\\ uU+p\xi_x\\ vU+p\xi_y\end{bmatrix};\ \hat{F}=\frac{1}{J}\begin{bmatrix}V-\eta_t\\ uV+p\eta_x\\ vV+p\eta_y\end{bmatrix} \tag{2}$$

and the viscous flux vectors, $\hat{E}_v$ and $\hat{F}_v$ are given as

$$\hat{E}_v=\frac{1}{J\,\mathrm{Re}}\begin{bmatrix}0\\ (\nabla\xi\cdot\nabla\xi)\,u_\xi+(\nabla\xi\cdot\nabla\eta)\,u_\eta\\ (\nabla\xi\cdot\nabla\xi)\,v_\xi+(\nabla\xi\cdot\nabla\eta)\,v_\eta\end{bmatrix}$$
$$\hat{F}_v=\frac{1}{J\,\mathrm{Re}}\begin{bmatrix}0\\ (\nabla\eta\cdot\nabla\xi)\,u_\xi+(\nabla\eta\cdot\nabla\eta)\,u_\eta\\ (\nabla\eta\cdot\nabla\xi)\,v_\xi+(\nabla\eta\cdot\nabla\eta)\,v_\eta\end{bmatrix} \tag{3}$$

Here J is the Jacobian of transformation and U and V are contravarient velocity components. Eq. (1) is numerically solved by iterative time marching scheme(Park et al., 1991, 1993).

To capture the turbulent flows, low Reynolds number k-ε model of Chien(1982) is employed.

$$\begin{aligned}&\frac{\partial}{\partial\tau}\left(\frac{k}{J}\right)+\frac{\partial}{\partial\xi}\left(U\frac{k}{J}\right)+\frac{\partial}{\partial\eta}\left(V\frac{k}{J}\right)\\ &=\frac{\partial}{\partial\xi}\left[\frac{\mu_k}{J}(\xi_x m_x+\xi_y m_y)\right]\\ &\quad+\frac{\partial}{\partial\eta}\left[\frac{\mu_k}{J}(\eta_x m_x+\eta_y m_y)\right]+\frac{P}{J}-\frac{\varepsilon}{J}-\frac{D}{J}\end{aligned} \tag{4}$$

$$\begin{aligned}&\frac{\partial}{\partial\tau}\left(\frac{\varepsilon}{J}\right)+\frac{\partial}{\partial\xi}\left(U\frac{\varepsilon}{J}\right)+\frac{\partial}{\partial\eta}\left(V\frac{\varepsilon}{J}\right)\\ &=\frac{\partial}{\partial\xi}\left[\frac{\mu_\varepsilon}{J}(\xi_x n_x+\xi_y n_y)\right]\\ &\quad+\frac{\partial}{\partial\eta}\left[\frac{\mu_\varepsilon}{J}(\eta_x n_x+\eta_y n_y)\right]\\ &\quad+\frac{C_1}{J}\frac{\varepsilon}{J}P-\frac{C_2}{J}f\frac{\varepsilon^2}{k}-\frac{E}{J}\end{aligned} \tag{5}$$

where

$$\mu_k=\frac{1}{\mathrm{Re}}+\frac{\nu_T}{\sigma_k},\ \mu_\varepsilon=\frac{1}{\mathrm{Re}}+\frac{\nu_T}{\sigma_\varepsilon}$$
$$m_x=\xi_x\frac{\partial k}{\partial\xi}+\eta_x\frac{\partial k}{\partial\eta},\ m_y=\xi_y\frac{\partial k}{\partial\xi}+\eta_y\frac{\partial k}{\partial\eta}$$
$$n_x=\xi_x\frac{\partial\varepsilon}{\partial\xi}+\eta_x\frac{\partial\varepsilon}{\partial\eta},\ n_y=\xi_y\frac{\partial\varepsilon}{\partial\xi}+\eta_y\frac{\partial\varepsilon}{\partial\eta}$$
$$D=\frac{2k}{y^2\mathrm{Re}},\ E=2\frac{\varepsilon}{y^2\mathrm{Re}}e^{-[\mathrm{Re}C_4u_*y]}$$

and P is the production of turbulence kinetic energy. u_* is the friction velocity defined as $u_*=\sqrt{\tau_w/\rho}$ and f is the wall dissipation function expressed as

$$f=1-\frac{0.4}{1.8}e^{-(\mathrm{Re}k^2/6\varepsilon)^2} \tag{6}$$

The turbulent eddy viscosity, ν_t is expressed as a function of the turbulence kinetic energy, k and dissipation rate of turbulence energy, ε.

$$\nu_t=C_\mu\frac{k^2}{\varepsilon}[1-e^{-(\mathrm{Re}C_3u_*y)}] \tag{7}$$

The empirical constants are given as;

$C_\mu=0.09$, $C_1=1.35$, $C_2=1.8$, $C_3=0.0115$, $C_4=0.5$, $\sigma_k=1.0$, $\sigma_\varepsilon=1.3$

The spatial derivatives of convective flux terms are obtained with third order accurate upwind

SMART (Sharp and Monotonic Algorithm for Realistic Transport, Gaskell et al., 1988) scheme to reduce unphysical oscillations for high Reynolds number flows, and the spatial derivatives of viscous terms and continuity equation are obtained with central differencing. The fourth order artificial damping term is added to the continuity equation to stabilize the present procedure.

2.2 Pollutant particle dispersion analysis

To predict particle dispersion, the present work assumes that

(1) Air pollutant is non-buoyant, preservative passive scalar which is dispersed in the homogeneous turbulent air flow.

(2) Specific gravity of pollutant is ignored.

(3) In streamwise direction, the effect of advection is dominant over diffusion. Thus, the streamwise diffusion is neglected.

(4) Concentration source is an infinite line source.

With above assumptions, the governing equation of pollutant dispersion in a generalized curvilinear two-dimensional coordinate system is described as follows;

$$\frac{\partial}{\partial\tau}\left(\frac{C}{J}\right)+\frac{\partial}{\partial\xi}\left(U\frac{C}{J}\right)+\frac{\partial}{\partial\eta}\left(V\frac{C}{J}\right)=\frac{\partial}{\partial\xi}\left[\frac{\xi_y}{J}(-\overline{v'c'})\right]+\frac{\partial}{\partial\eta}\left[\frac{\eta_y}{J}(-\overline{v'c'})\right]+\frac{Q(\xi,\eta)}{J} \tag{8}$$

where C is the mean concentration of the air pollutant. The bar over primed quantities means time average of fluctuation. The source strength function Q is expressed by a dirac delta function and has the dimension of [mass/(volume·time)]. Using the gradient diffusion theory (called K-theory, Dyer, 1974), Eq. (8) can be rewritten as;

$$\frac{\partial}{\partial\tau}\left(\frac{C}{J}\right)+\frac{\partial}{\partial\xi}\left(U\frac{C}{J}\right)+\frac{\partial}{\partial\eta}\left(V\frac{C}{J}\right)=\frac{1}{\mathrm{Re}}\left\{\frac{\partial}{\partial\xi}\left[K_\eta\xi_y\left(\frac{\partial}{\partial\xi}\left\langle\frac{\xi_y C}{J}\right\rangle+\frac{\partial}{\partial\eta}\left\langle\frac{\eta_y C}{J}\right\rangle\right)\right]\right\}+\frac{1}{\mathrm{Re}}\left\{\frac{\partial}{\partial\eta}\left[K_\eta\eta_y\left(\frac{\partial}{\partial\xi}\left\langle\frac{\xi_y C}{J}\right\rangle+\frac{\partial}{\partial\eta}\left\langle\frac{\eta_y C}{J}\right\rangle\right)\right]\right\}+\frac{Q(\xi,\eta)}{J} \tag{9}$$

where K_η is the turbulent eddy diffusivity in η-direction, which is related with the Reynolds analogy;

$$K_\eta=\frac{\nu_t}{Sc_t} \tag{10}$$

where Sc_t is the turbulent Schmidt number, 0.7 is used in this study.

2.3 Initial and boundary condition

The inflow boundary condition is imposed as

$$u=\begin{cases}\dfrac{u_*}{\kappa}\ln\dfrac{y}{y_0} & \text{for } y\le\delta\\ u_\infty & \text{for } y>\delta\end{cases}\qquad v=0 \tag{11}$$

where δ is the boundary thickness and κ is the von-Karman constant and y_0 is the surface roughness height respectively. The kinetic energy and dissipation rate of turbulence at inlet are given as

$$k=\begin{cases}C_\mu^{-1/2}u_*^2\left(1-\dfrac{y}{\delta}\right)^2 & \text{for } y\le 0.9\delta\\ k_\infty & \text{for } y>0.9\delta\end{cases}\qquad \varepsilon=\frac{C_\mu^{3/4}k^{3/2}}{\kappa y} \tag{12}$$

On the solid surface, no slip condition is imposed for velocity components. The surface pressure distribution is determined by setting the normal gradient of pressure to be zero. The kinetic energy and dissipation rate of turbulence on the solid surface are set to zero. The concentration, C, is initially set to zero in whole computational domain except at the location of source, where the pollutant continuously emits from $t=0$ by an amount of source strength, Q.

3. Results and Discussion

3.1 Flat plate

For the code validation, the present procedure has been applied to the particle dispersion emitted from an elevated line source over the flat plate, which was previously measured by Raupach et al. (1983). Figure 1 shows the mean velocity profile, compared with experiment.

Figure 3 shows the mean concentration profiles at four downstream locations as shown in Fig. 2. The agreement is fairly good except in the

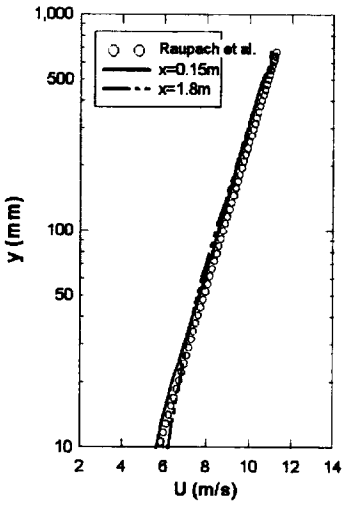

Fig. 1 Velocity profile over the flat plate

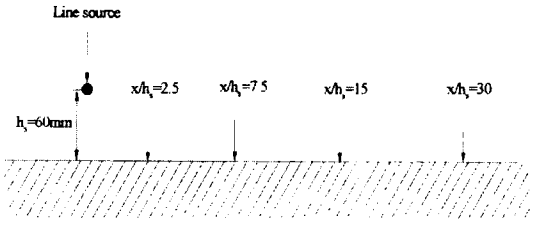

Fig. 2 Schematic of location of source and measurements

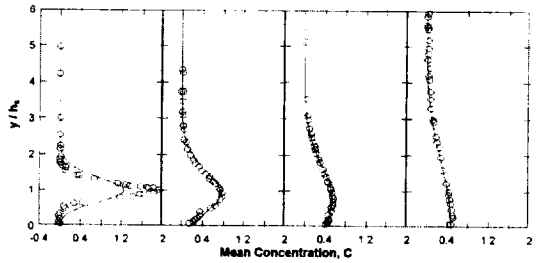

(a) at $x/h_s=2.5$ (b) at $x/h_s=7.5$ (c) at $x/h_s=15$ (d) at $x/h_s=30$

Fig. 3 Pollutant concentration profiles at several locations (○: Experiment (Raupach et al., 1983), —: Present)

vicinity of source, i.e., near $y=h_s$ of Fig. 3(a). This underestimate near the source is known as one of common defects of the gradient diffusion theory in turbulent flows(Raupach et al., 1983). The mean ground-level concentration (GLC) along x-axis is shown in Fig. 4 that shows also good agreement with experiment.

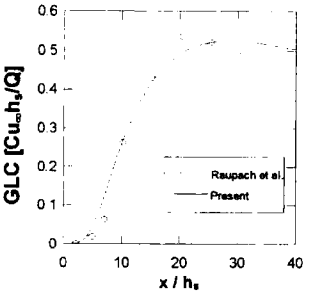

Fig. 4 Ground level concentration(GLC) distribution along x-axis

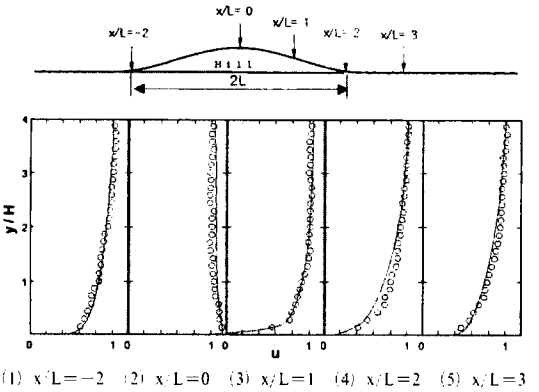

(1) x/L=−2 (2) x/L=0 (3) x/L=1 (4) x/L=2 (5) x/L=3

(a) Horizontal velocity component

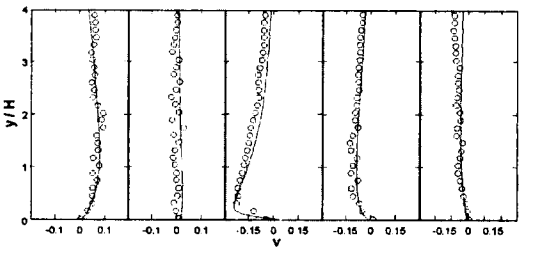

(1) x/L=−2 (2) x/L=0 (3) x/L=1 (4) x/L=2 (5) x/L=3

(b) Vertical velocity component

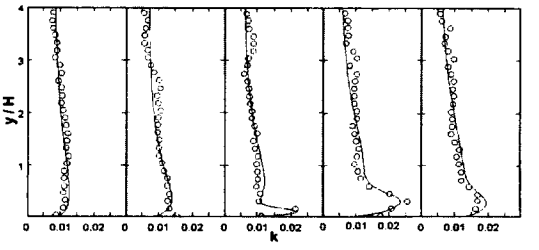

(1) x/L=−2 (2) x/L=0 (3) x/L=1 (4) x/L=2 (5) x/L=3

(c) Turbulent kinetic energy

Fig. 5 Velocity and turbulent kinetic energy profiles over the cosine-shaped hill ($A=3/7$) (○: Experiment (Kim et al., 1997a), —: Present)

3.2 Cosine-shaped hill

The present numerical model has been also applied to two 2-D cosine-shaped hills, having aspect ratios of 3/7 and 3/4. The aspect ratio, Λ is defined as $\Lambda=a/H$, where a is the half length of the hill base and H is the hill height. Figure 5 shows the velocity and turbulent kinetic energy profiles at several locations compared with experiment (Kim et al., 1997a).

Figure 6 shows the fractional speed-up ratio which is defined as

$$\Delta S=\frac{u(y)-u_0(y)}{u_0(y)} \tag{13}$$

where $u(y)$ is the amplified wind speed and $u_0(y)$ is the speed of the approaching wind at the same height above the ground. As shown in the figure, the present numerical model predicts well a maximum fractional speed-up ratio whose value is 1.2 at B-location, i.e., at the summit of a hill.

Figure 7 shows the distribution of surface pressure coefficient over the cosine-shaped hill. Figure 8 shows the distributions of ground level concentrations of two different emission heights of h_s=0.5 H and h_s=1.0 H, compared with other numerical data (Kim et al., 1997a). It is found that the present result has a good agreement with the other numerical data.

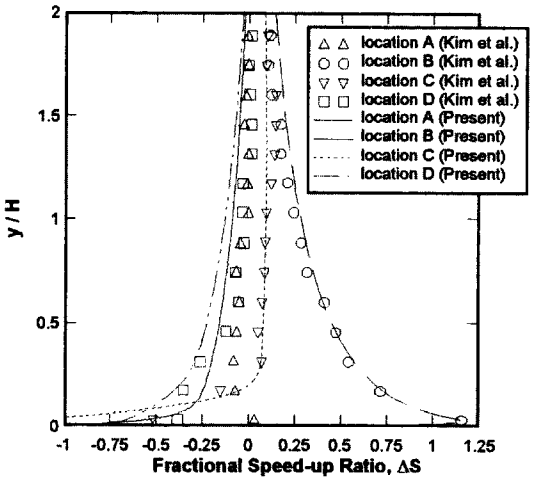

Fig. 6 Fractional speed-up ratio (Λ=3/7)

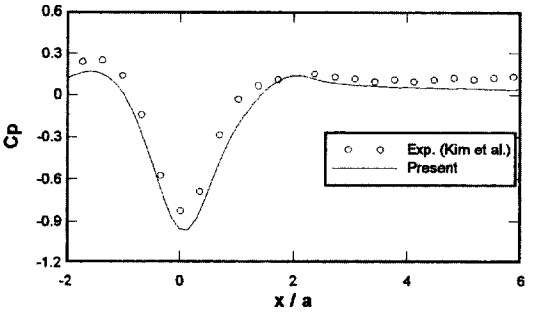

Fig. 7 Surface pressure distribution on the cosine-shaped hill (Λ=3/7)

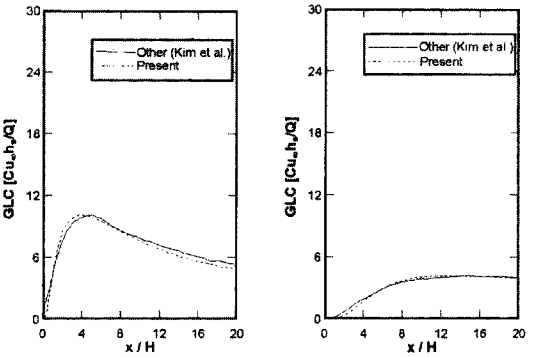

(a) Source height : h_s=0.5 H (b) Source height : h_s=1.0 H

Fig. 8 Ground level concentration of two different source heights (Λ=3/4)

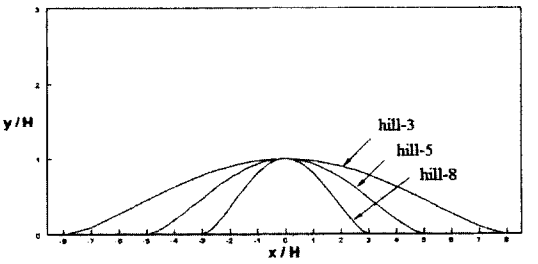

(a) Topographic profile

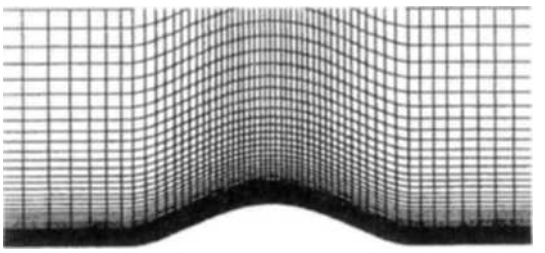

(b) Grid system(hill-3)

Fig. 9 Topographic profile and grid systen of the Russian hills

3.3 Russian hill

This Russian hill has a profile given by

$$x=\frac{1}{2}\chi\left[1+\frac{a^2}{\chi^2+m^2(a^2-\chi^2)}\right]$$
$$y=\frac{1}{2}m\sqrt{a^2-\chi^2}\left[1-\frac{a^2}{\chi^2+m^2(a^2-\chi^2)}\right] \quad (14)$$

where $|\chi|\leq a$ and $m=\Lambda^{-1}+\sqrt{\Lambda^{-2}+1}$. In the present work, three Russian hills having different aspect ratio as shown in Fig. 9 are computed. The hill-3, 5, and 8 denote that the aspect ratio are 3, 5, and 8, respectively.

Figures 10-12 are the velocity profiles, compared with the experiment (Gong, 1991) and shows good agreement with each other. Figure 13 shows the streamlines over the hills. The hill-3,

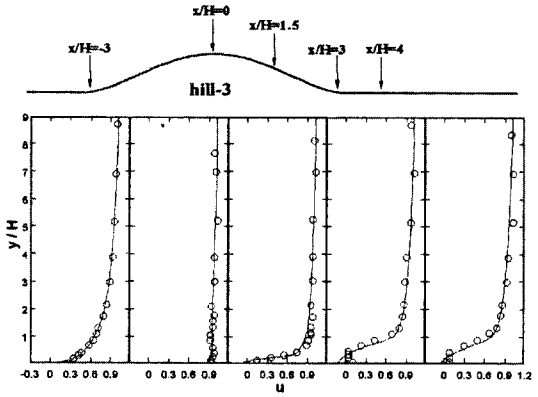

(a) x/H=−3 (b) x/H=0 (c) x/H=1.5 (d) x/H=3 (e) x/H=4

Fig. 10 Velocity profile over the hill-3 (○: Experiment (Gong, 1991), —: Present)

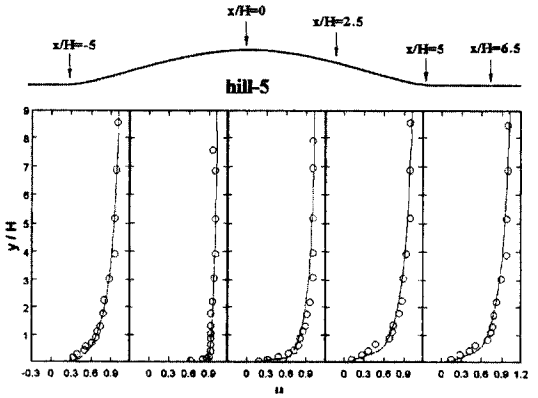

(a) x/H=−5 (b) x/H=0 (c) x/H=2.5 (d) x/H=5 (e) x/H=6.5

Fig. 11 Velocity profile over the hill-5 (○: Experiment (Gong, 1991), —: Present)

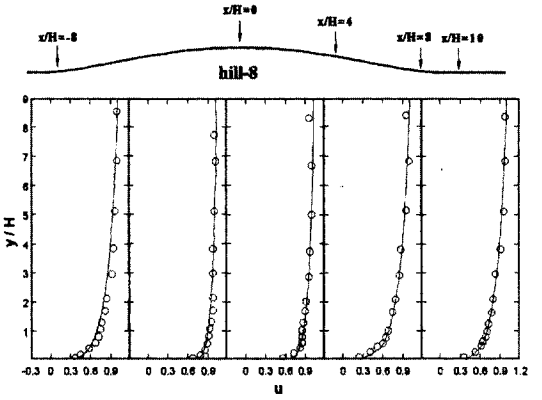

(a) x/H=−8 (b) x/H=0 (c) x/H=4 (d) x/H=8 (e) x/H=10

Fig. 12 Velocity profile over the hill-8 (○: Experiment (Gong, 1991), —: Present)

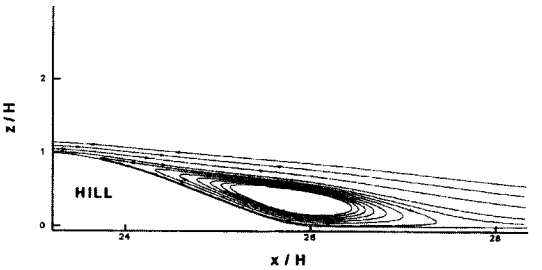

(a) Over the hill-3

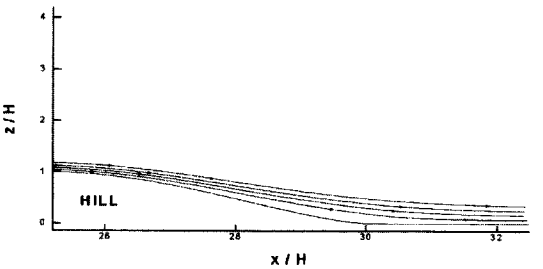

(b) Over the hill-5

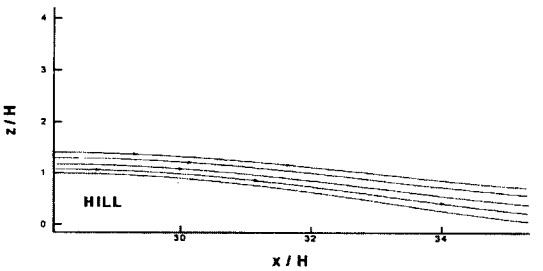

(c) Over the hill-8

Fig. 13 Streamlines over the Russian hills

the steepest hill, has a separated flow region in the leeward side, while two hills have not. The length of separated region is about 5.4 H that agrees well with the measured value of 5.5 H. Figure 14 shows the Reynolds shear stress over the hill-3 which is the worst case of analyzing turbulent flow with k-ε model because of a massive separated flow region.

The speed-up ratio, defined as Eq. (13), is represented in Fig. 15 and, as expected, the speed-up ratio increases with the decrease in aspect ratio of a hill.

Figures 16-18 illustrate the mean pollutant concentration contours, normalized by the source strength. In Fig. 16 of the hill-3, the pollutant is, consequently, spread strongly even in the upwind direction from the source, since the source height of 0.25 H and 0.5 H are located inside of recirculated flow region.

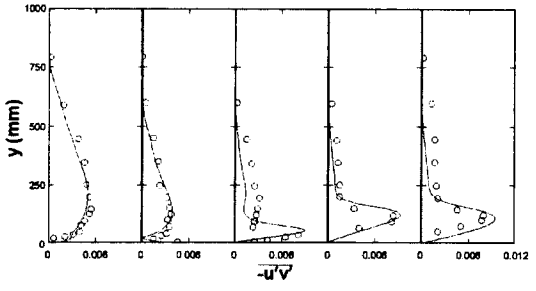

(a) x/H=-3 (b) x/H=0 (c) x/H=1.5 (d) x/H=3 (e) x/H=4

Fig. 14 Normalized Reynolds stress profile over the hill-3 (○: Experiment (Gong, 1991), —: Present)

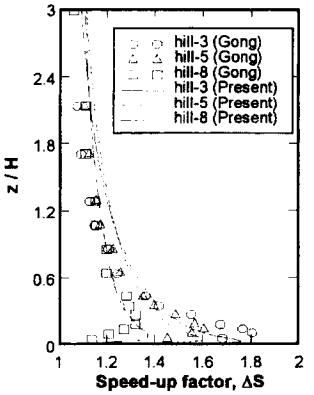

Fig. 15 Speed-up ratio compared with experiment

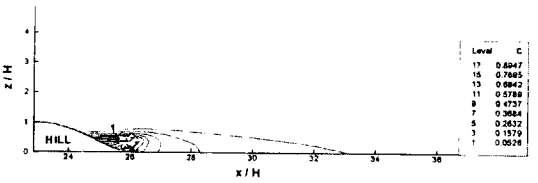

(a) Source height : h_s=0.25 H

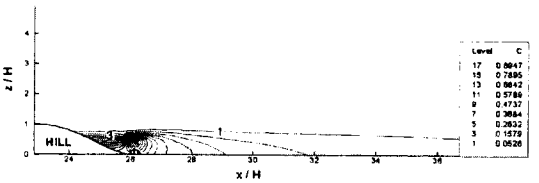

(b) Source height : h_s=0.5 H

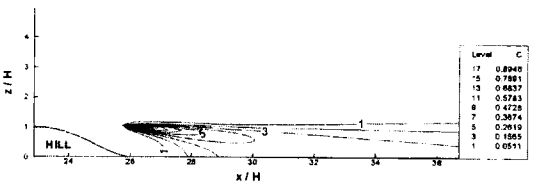

(c) Source height : h_s=1.0 H

Fig. 16 Pollutant concentration contours over the hill-3 in case of three different source heights

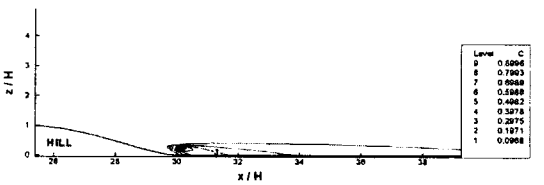

(a) Source height : h_s=0.25 H

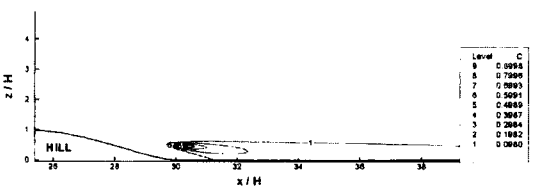

(b) Source height : h_s=0.5 H

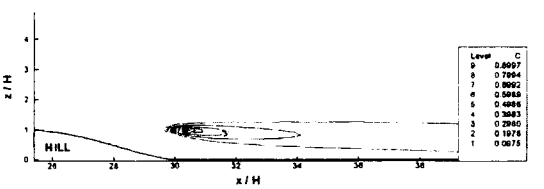

(c) Source height : h_s=1.0 H

Fig. 17 Pollutant concentration contours over the hill-5 in case of three different source heights

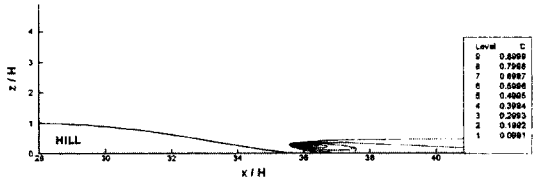

(a) Source height : h_s=0.25 H

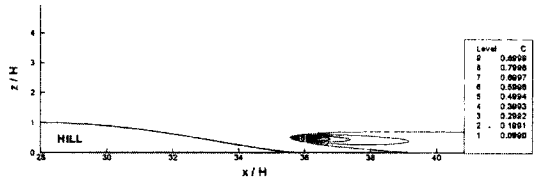

(b) Source height : h_s=0.5 H

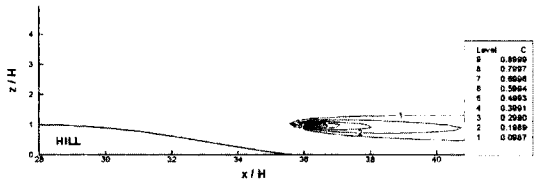

(c) Source height : h_s=1.0 H

Fig. 18 Pollutant concentration contours over the hill-8 in case of three different source heights

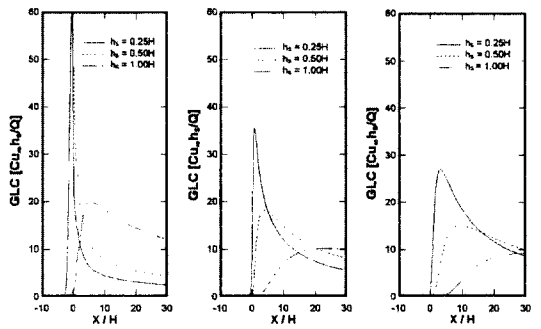

(a) Hill-3 (b) Hill-5 (c) Hill-8

Fig. 19 Ground level concentration (GLC) distribution

Figure 19 shows the ground level concentration (GLC) distribution along the x-axis. The maximum GLC decreases sharply with increasing source height in all cases and is strongly influenced by the aspect ratio of the hill, especially whether the source is located inside of separated region or not. The peak concentrations are greatly enhanced by the presence of the hill, which can be characterized by Terrain Amplification Factor (TAF). The TAF is defined as the ratio of the maximum GLC in the presence of the hill to that in the absence of the hill. Thus, the TAF will depend on the hill shape and aspect ratio, as well as the location and height of the source. The TAF for the present hill aspect ratios and source heights is given in Table. 1.

Table 1 Terrain Amplification Factor(TAF) of the Russian hill

Hill aspect ratio	Source height	TAF
3	0.25 H	5.50
	0.50 H	7.51
	1.00 H	3.45
5	0.25 H	3.26
	0.50 H	2.23
	1.00 H	1.76
8	0.25 H	2.49
	0.50 H	1.86
	1.00 H	1.64

4. Conclusions

A computer code for predicting atmospheric wind flow field and pollutant dispersion over the hilly terrain has been successfully developed. The present code uses the Reynolds averaged Navier-Stokes equation and the gradient diffusion theory (K-theory) as the governing equations. The code validation has been assessed by comparison of velocity, turbulent kinetic energy, Reynolds shear stress, speed-up ratio, and ground level concentration with various experimental and numerical data. Good agreement has been achieved. From the present calculation, it has been found that the pollutant concentration and ground level concentration have been strongly influenced with the hill shape and aspect ratio, as well as the location and height of the source. Especially, when the source is located within the flow separated region, the pollutant particles disperse even upstream direction and the maximum ground level concentration near the source increases dramatically.

Acknowledgment

This work had been sponsored by Korea Science and Engineering Foundation(KOSEF) and Advanced Ship Engineering Research Center (ASERC). The authors would like to appreciate KOSEF and ASERC for the financial support of this work.

References

Arya, S. P. S., Capuano, M. E. and Fagen, L. C., 1987, "Some Fluid Modeling Studies of Flow and Dispersion over Two-Dimensional Low Hills," *Atmospheric Environment*, Vol. 21, No. 4, pp. 753~764.

Castro, I. P. and Apsley, D. D., 1997, "Flow and Dispersion over Topography : A Comparison Between Numerical and Laboratory Data for Two-Dimensional Flows," *Atmospheric Environment*, Vol. 31, No. 6, pp. 839~850.

Chien, K. Y., 1982, "Prediction of Channel and Boundary-Layer Flows with a Low-Reynolds Number Turbulent Model," *AIAA Journal*, Vol. 20, No. 1, pp. 33~38.

Dyer, A. J., 1974, "A Review of Flux-profile Relationships," *Boundary-Layer Meteorology*, Vol. 7.

Gaskell, P. H. and Lau, A. K. C., 1988, "Curvature-Compensated Convective Transport : SMART, a New Boundedness-Preserving Transport," *International Journal for Numerical Methods in Fluids*, Vol. 8, pp. 617~641.

Gong, W. and Ibbetson, A., 1989, "A Wind Tunnel Study of Turbulent Flow over Model Hills," *Boundary-Layer Meteorology*, Vol. 49, pp. 113~148.

Gong, W., 1991, "A Wind Tunnel Study of Turbulent Dispersion over Two- and Three-Dimensional Gentle Hills from Upwind Point Sources in Neutral Flow," *Boundary-Layer Meteorology*, Vol. 54, pp. 211~230.

Kim, H. G., Lee, C. M., Lim, H. C. and Kyong, N. H., 1997a, "An Experimental and Numerical Study on the Flow over Two-dimensional Hills," *Journal of Wind Engineering and Industrial Aerodynamics*, Vol. 66, pp. 17~33.

Kim, H. G. and Lee, C. M., 1997b, "Numerical Analysis of the Two-Dimensional Pollutant Dispersion Over Hilly Terrain," *Journal of Korea Air Pollution Research Association*, Vol. 13, No. 5, pp. 383~396. (in Korean)

Park, W. G. and Sankar, L. N., 1991, "An Iterative Time Marching Procedure for Unsteady Viscous Flows," *ASME-BED*, Vol. 20, pp. 281~284.

Park, W. G. and Sankar, L. N., 1993, "A Technique for the Prediction of Unsteady Incompressible Viscous Flows," *AIAA Paper* 93-3006.

Raupach, M. R. and Legg, B. J., 1983, "Turbulent Dispersion from an Elevated Line Source : Measurement of Wind-Concentration Moments and Budgets," *Journal of Fluid Mechanics*, Vol. 136, pp. 11~137.

Robert, P. T., Fryer-Taylor, R. E. J., 1994, "Wind Tunnel Studies of Roughness Effects in Gas Dispersion," *Atmospheric Environment*, Vol. 28, No. 11, pp. 1861~1870.